Quark-bag nontopological solitons with good four-momentum. II. Calculations of the soliton rest mass

H. R. Fiebig*
Department of Physics, State University of New York, Stony Brook, New York 11794

E. Hadjimichael
Department of Physics, Yale University, New Haven, Connecticut 06515
and Department of Physics, Fairfield University, Fairfield, Connecticut 06430†

(Received 30 September 1983)

In the preceding paper, how to construct soliton-bag-model states with good four-momentum was shown. Here these states are utilized in a model calculation of the soliton rest mass M. How to employ a variational procedure for evaluating the energy of the system is also demonstrated. The results are examined with respect to the parameters of the model. In a calculation of the rest mass of the Ω^- baryon we include phenomenological gluonic corrections.

I. INTRODUCTION

Bag models seem now to be firmly established as tools for the nuclear physicist as well as for the particle physicist.[1,2] While the fixed-cavity approximation to bag models finds widespread applications, it does violate Poincaré invariance and leads to the need for relativistic corrections. Hence, many authors have recently devoted their work to estimates of recoil effects or to a cure for the violation of translational invariance.[3,4] This aspect is relevant even if one is only interested in static properties such as baryon masses and magnetic moments; calculations reveal errors ranging from 10 to 30%. Translational invariance undoubtedly requires careful consideration if one examines processes involving high momentum transfer to the baryon, say $q \gtrsim mc$, where the bag recoils in the final state.

In a preceding paper[5] (subsequently referred to as I) we have worked out a theoretical basis for the construction of bag-model states with good total four-momentum. We argued that the (so-called) soliton model of Friedberg and Lee[6] was a suitable framework to apply a relativistic version of the Peierls-Yoccoz[7] momentum-projection technique. As a result we now have available bag-model states that are rigorously free from the ambiguities due to spurious center-of-mass excitations which plague the fixed-cavity approach.

In this paper we take the first step toward applying the formalism developed in I. We focus here on calculations of the rest mass M of a Friedberg-Lee soliton. The combined system of the quarks and the bag itself constitutes a complicated many-body problem. To deal with it, a variational procedure directly applicable to the many-body Hamiltonian matrix elements with trial functions both for the quark spinors and the σ field, i.e., the bubble (or bag), turns out to be most feasible. This approach is not only numerically easier than actually solving the (coupled, one-body) equations of motion of the Friedberg-Lee model; it is also conceptually pleasing because the variation is performed *after* the momentum projection.

This paper is organized as follows. In Sec. II we briefly review some essential parts of the formalism developed in the previous work that is relevant to the task at hand. In Sec. III we describe our choice for the trial functions for the quark spinors and the vacuum bubble (σ field) and also explain details of the variational method employed to evaluate the soliton rest mass. Finally, Sec. IV is devoted to the presentation and discussion of our results.

II. REVIEW OF THEORETICAL FRAMEWORK

The Friedberg-Lee soliton model is based on the Lagrangian

$$\mathscr{L}=\frac{i}{2}\bar{\psi}\overleftrightarrow{\partial}\psi-\bar{\psi}(m_q+g\sigma)\psi+\tfrac{1}{2}(\partial\sigma)^2-V(\sigma)\ . \tag{1}$$

Here ψ and m_q are the quark field and its bare mass, respectively, σ is a Lorentz-scalar field, and g is a dimensionless coupling constant. The "potential" $V(\sigma)$, which is usually taken to have a quartic form, i.e.,

$$V(\sigma)=p+\frac{a}{2}\sigma^2+\frac{b}{6}\sigma^3+\frac{c}{24}\sigma^4\ , \tag{2}$$

determines the physics described by the model. $V(\sigma)$ has two local minima at $\sigma=0$ and $\sigma=f>0$ with $V(0)=p>0$ and $V(f)=0$, respectively (see Fig. 1 of I). Further σ is assumed to contain a static background field $\sigma_{\rm st}$. The latter simulates the color-dia-electric properties of the vacuum $|v\rangle$ and essentially provides the bubble (bag) in which the quarks reside.

The (nontopological) soliton-model state with good four-momentum K is built on the vacuum $|v\rangle$ in the following way:

$$|B(K)\rangle=N_B{}^{-1}\Pi_K U(\Lambda_K)B^\dagger|v\rangle\ . \tag{3}$$

The Fock-space operator $B^\dagger$ creates quarks, say three for a baryon, with appropriately coupled color-flavor-spin quantum numbers. Thus $B^\dagger|v\rangle$ describes three quarks in a bubble, with average momentum equal to zero (rest frame). In I we have shown how to construct a unitary operator $U(\Lambda_K)$ associated with a Lorentz boost Λ_K, i.e.,

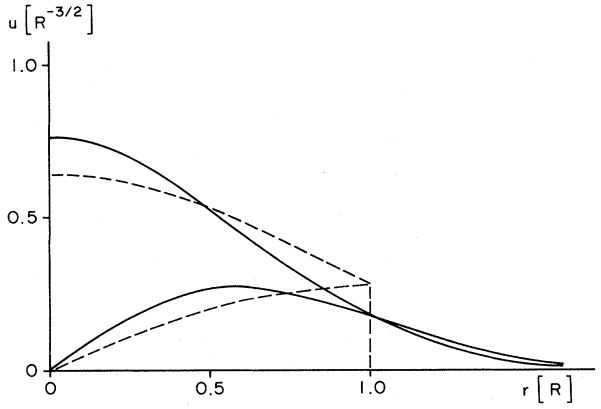

FIG. 1. The upper and lower components of the quark spinor employed in this work, Eq. (14a) (solid curves) compared to the corresponding MIT bag quantities (dashed curves).

$$(M,\vec{0}) \underset{\Lambda_K}{\rightarrow} (K^0,\vec{K}) , \tag{4}$$

where M is the rest mass of the entire system. Hence $U(\Lambda_K)B^\dagger|v\rangle$ is a state with average four-momentum K. Finally the operator Π_K with

$$\Pi_{K'}\Pi_K=\delta^4(K'-K)\Pi_K \tag{5}$$

projects out the good four-momentum K. (See I for exact expression for Π_K.) The normalization constant N_B is given by

$$N_B{}^2=\langle v|B\Pi_{(M,\vec{0})}B^\dagger|v\rangle \tag{6}$$

and only depends on intrinsic properties of the model soliton. Using the model state (3), we derived a formula for the soliton rest mass

$$M=\frac{\langle v|BH\Pi_{(M,\vec{0})}B^\dagger|v\rangle}{\langle v|B\Pi_{(M,\vec{0})}B^\dagger|v\rangle} . \tag{7}$$

Here the mass M appears on both sides of the equation. Therefore, it is clear that we are dealing with a self-consistency problem. The Hamiltonian H is derived from the model defining Lagrangian (1). We choose to split H into four parts

$$H=H_{\rm DIR}+H_{\rm SIG}+H_{\rm CPL}+H_{\rm POT} \tag{8a}$$

with

$$H_{\rm DIR}=\int d^3x:\bar{\psi}(x)\left[-\frac{i}{2}\vec{\gamma}\cdot\overleftrightarrow{\nabla}+m_q\right]\psi(x): \tag{8b}$$

$$H_{\rm SIG}=\int d^3x:\{\dot{\sigma}(x)^2+[\vec{\nabla}\sigma(x)]^2\}: \tag{8c}$$

$$H_{\rm CPL}=g\int d^3x:\bar{\psi}(x)\sigma(x)\psi(x): \tag{8d}$$

$$H_{\rm POT}=\int d^3x:V(\sigma(x)): \tag{8e}$$

These are the Dirac energy, the σ-field energy, the coupling energy, and the potential energy, respectively.

The fields ψ and σ are expanded in terms of Fock-space operators in the Heisenberg picture, i.e.,

$$\psi(x)=\sum_k[u_k(x)b_k+v_k(x)d_k^\dagger] \tag{9}$$

with time-independent spinors $u_k(\vec{x})$ and $v_k(\vec{x})$. The latter are assumed to be normalizable in order to reflect the localized nature of the quark distribution. The σ field is written as

$$\sigma(x)=f+\sum_{n=1}^{N}(2\epsilon_n)^{-1/2}\phi_n(x)(s_n+s_n^\dagger)+\sigma_{\rm fl}(x) . \tag{10}$$

Here we encounter a subtlety. The sum over n in (10) is the quasiclassical part in the sense explained in I. The Fock-space operators s_n are time independent and the ϵ_n are arbitrary energies, for $n\leq N$. The time-dependent pieces are contained in the quantum-fluctuation part $\sigma_{\rm fl}(x)$. We use (10) to make an ansatz for the vacuum bubble, i.e., the coherent-state approximation[8]

$$|v\rangle=e^{-\chi^2/2}\exp(-\chi s_1^\dagger)|0\rangle , \tag{11}$$

where $|0\rangle$ is the normal (translationally invariant) vacuum and χ is a parameter. Because of this ansatz we will only be concerned with the $n=1$ term in the expansion (10). Thus, in the present application, ϵ_1 sets the energy scale for the soliton system and $\phi_1(\vec{x})$ describes the geometrical shape of the static vacuum bubble.

The spinors $u_k(\vec{x}),v_k(\vec{x})$ and the vacuum function $\phi_n(\vec{x})$ in the expansions (9) and (10), respectively, are to be determined by the dynamics based on the Lagrangian (1). In the present context, the solutions of the (coupled nonlinear) equations of motion, Eqs. (4) of I, for just single-particle wave functions are of limited use. There are two main reasons. First, because of the nonlinear nature of the Friedberg-Lee model, solutions of a many-body problem cannot be constructed rigorously from a superposition of one-body solutions. Second, applying a momentum-projection operator requires analytical manipulations of the wave functions. If these were available in numerical form only (which is the best we can hope for, given the complexity of the equations of motion), their practical usefulness would be questionable. Therefore our point of view here is that for both conceptual and practical reasons it is best to tackle the many-body problem directly. This means in particular that we apply a variational principle directly to the many-body matrix elements of the Hamiltonian in the momentum-projected basis. The wave functions of the quark and vacuum modes populated in (3) are taken to be *trial functions* suited to the physical situation. They are supposed to depend on variational parameters and they should also have a convenient analytical structure in order to make the evaluation of the matrix elements in the momentum-projected basis feasible.

In I we have derived formulas for the normalization and the four pieces $H_{\rm DIR},H_{\rm SIG},H_{\rm CPL},H_{\rm POT}$ of the Hamiltonian matrix elements in terms of contractions between Fock-space operators. These contractions involve the trial functions just mentioned. Thus, the results in I can be directly used here with a particular choice of trial functions as we shall see in the next section.

III. THE VARIATIONAL CALCULATION

A. Parameters

Let us first discuss the parameters of the soliton model. In the defining equations (1) and (2) we encounter the constants m_q,g and c,b,a,p. Furthermore f is the expectation value of the σ field in the normal vacuum. The potential has the properties $V(0)=p$, $V'(0)=0$, and additionally we require $V(f)=V'(f)=0$. Using the latter two conditions we can replace c,b,a with one parameter; let us choose it to be m_σ, i.e., the bare mass of the σ field. At the normal vacuum $\sigma=f$, we have $V''(f)={m_\sigma}^2$. In terms of the new parameter, the potential (2) reads

$$V(\sigma)=V_{\rm INF}(\sigma)+V_{\rm FIN}(\sigma) \tag{12a}$$

with

$$V_{\rm INF}(\sigma)=\tfrac{1}{2}{m_\sigma}^2(\sigma-f)^2\left[1+\frac{2}{f}(\sigma-f)+\frac{1}{f^2}(\sigma-f)^2\right], \tag{12b}$$

$$V_{\rm FIN}(\sigma)=-\frac{4p}{f^2}(\sigma-f)^3-\frac{3p}{f^4}(\sigma-f)^4 . \tag{12c}$$

Note that $V_{\rm INF}(\sigma)$ is explicitly a function of ${m_\sigma}^2$. The usefulness of this separation will become evident later.

The second derivative at $\sigma=0$ turns out to be $V''(0)={m_\sigma}^2-12pf^{-2}$; we require its positivity as an additional constraint. Since our model is supposed to describe a situation where quantum fluctuations of the σ field are practically negligible,[5] the σ mass m_σ must be very large as compared to a typical energy scale.

In addition, the coupling term in (1) entails that quarks which penetrate into the normal vacuum, i.e., $\sigma=f$, acquire an additional mass gf. In order to achieve quark confinement this *outside-quark* mass gf must become large as compared to a typical energy scale.

Actually we would like to go to the exact limits of infinite σ and outside-quark masses. Since f remains finite, this means that $m_\sigma\to\infty$ and $g\to\infty$. The rates at which m_σ and g go to infinity must however be related. From Eqs. (8d) and (12b) we find that the potential contains a term proportional to ${m_\sigma}^2$ and the coupling term is proportional to g. We must therefore achieve the limit so that $g/{m_\sigma}^2$ remains finite. For this purpose we define the dimensionless parameter

$$y=\frac{gf}{{m_\sigma}^2/\epsilon_1} , \tag{13}$$

where ϵ_1 is the energy unit for our soliton system.

The soliton model describes a variety of distinct bag models depending on the choice of the different parameters. It is interesting to note, for example, that in the limit $m_\sigma\to\infty$ we achieve the MIT bag condition. From Ref. 6 we learn that the quantities

$$n=Ag^2\epsilon^2/{m_\sigma}^2 ,$$

$$N=p/({m_\sigma}^2f^2)^{4/3} ,$$

where $\epsilon=2.04/R$ and $A=3$ or $A=2$, characterize a bag of radius R. A necessary condition for the MIT limit is $n\to\infty$ and $\lambda\to0$. Substituting our soliton model parameters, we discover that $n\sim{m_\sigma}^2$ and $\lambda\sim{m_\sigma}^{-8/3}$. Hence the limit $m_\sigma\to\infty$ coincides precisely with the above condition. It should be kept in mind however that even in the limit $m_\sigma\to\infty$, the soliton model is still more general than the MIT bag because the parameters f and y provide additional freedom.

B. Trial functions

The choice of the trial functions for the quark spinors and the vacuum bubble is critical for the quality of the results. On the other hand a simple analytical structure is also highly desirable for practical reasons. Our attitude here is to employ a variational ground-state trial spinor which is a close approximation to the exact MIT ground state, but on the other hand involves only functions of structure (Gaussian)$\times$(polynomial). Our choice is

$$u_{0s}(\vec{x})=n_0\begin{bmatrix}1\\ \dfrac{-i\vec{\sigma}\cdot\nabla}{(\omega_0+m_q)}\end{bmatrix}(\pi{b_0}^2)^{-3/4}e^{-\vec{x}^2/2{b_0}^2}u_s , \tag{14a}$$

$$n_0=\left[1+\frac{3/2}{(\omega_0+m_q)^2{b_0}^2}\right]^{-1/2} , \tag{14b}$$

where n_0 is a normalization constant and u_s a Pauli spinor. Both ω_0 and b_0 may be regarded as variational parameters.

The particular choice of the lower component in (14a) ensures that if we apply the Dirac operator, i.e.,

$$(i\partial\!\!\!/-m_q)u_{0s}(\vec{x})e^{-i\omega_0t} ,$$

the lower components of this quantity are identically zero. This statement does not depend on the specific Gaussian structure. It is essential to understand that the frequency ω_0 is a variational energy parameter and not necessarily the Dirac energy of the quarks. The upper component of $(i\partial\!\!\!/-m_q)u_{0s}(\vec{x})e^{-i\omega_0t}$ is not identically zero; we may require however that its $|\vec{x}|$ integral from 0 to ∞ be zero. This prescription of "satisfying the Dirac equation on the average" determines the width b_0 of the Gaussian,

$$b_0=\left[\frac{2}{{\omega_0}^2-{m_q}^2}\right]^{1/2} . \tag{14c}$$

Further, it is obvious that the Gaussian $\exp(-\vec{x}^2/2{b_0}^2)$ in (14a) plays the role of $j_0(2.04|x|/R)\theta(R-|\vec{x}|)$ which appears in the MIT spinor for a bag of radius R. In fact it is straightforward to relate b_0 to the MIT bag radius; applying the MIT boundary condition to (14a) yields

$$R=(\omega_0+m_q){b_0}^2 . \tag{15}$$

This relation is not an additional constraint because R and b_0 are interchangeable parameters. We may use (14c) and (15) to express ω_0 and b_0 in terms of R. For zero quark mass $m_q=0$, we obtain $b_0=R/\sqrt{2}$ and $\omega_0=2/R$. The latter frequency is astonishingly close to $2.04/R$, the MIT result (without self-energy corrections[1]). In Fig. 1 we compare, for this situation, the upper and lower com-

TABLE I. Model and variational parameters of the soliton model.

Model parameters	Trial parameters
m_q	χ
f	b_1
p	$M=E(M)$
$m_\sigma \to \infty$	
$g \to \infty$	

ponents of our Gaussian ansatz (14) to the corresponding quantities of the MIT bag. The discontinuity is, of course, not reproduced but merely approximated by the rapid dropoff of the Gaussian.

As a trial function for the vacuum bubble we also take a Gaussian

$$\phi_1(\vec{x})=(\pi b_1^2)^{-3/2}e^{-x^2/2b_1^2} \tag{16}$$

with a different width b_1 which is also regarded as a variational parameter.

It is of course understood that both (14) and (16) may be viewed as first terms of series expansions. For instance, substituting a sum over oscillator functions for the Gaussians in (14a) and (16) would be a natural generalization. Each expansion coefficient would then play the role of a new parameter.

We summarize in Table I the parameters of our model. One should note that there are two sets of parameters of distinct character. The model parameters appear in the Lagrangian and are given specific values. The trial parameters are determined as a result of the variational procedure.

C. Details of the variational procedure

Using the results of I, we are now in a position to calculate the matrix elements of the four pieces of the Hamiltonian (8). In the Appendix, these are listed as functions of ω_0, χ, b_0, and b_1. It is important to recall from I that because of the exponential time dependence $e^{-i\omega_0 t}$ and the momentum projection the matrix elements both in the numerator and the denominator of the expression (7) for the rest mass have factors $\delta(M-3\omega_0)$. Although these drop out from (7) their effect is that $\omega_0=M/3$ has to be substituted in all matrix elements. We therefore are left with the following parameter dependence:

$$E_X(M;\chi,b_1)=\frac{\langle v \mid BH_X\Pi_{(M,\vec{0})}B^\dagger \mid v\rangle}{\langle v \mid B\Pi_{(M,\vec{0})}B^\dagger \mid v\rangle} \tag{17}$$

for X=DIR, SIG, CPL, POT, etc. Note that b_0 was fixed by (14c), i.e., $b_0^2=2/(M^2/9-m_q^2)$.

Let us now consider the limit of infinite σ mass, $m_\sigma \to \infty$, as explained in Sec. III A. We recall that both $E_{\rm CPL}(M;\chi,b_1)$ and $E_{\rm INF}(M;\chi,b_1)$, Eq. (12), became infinite for $m_\sigma \to \infty$. In particular, the quantity

$$E_{\rm CON}(M;\chi,b_1)=E_{\rm CPL}(M;\chi,b_1)+E_{\rm INF}(M;\chi,b_1) \tag{18}$$

is proportional to m_σ^2. This means that the limit $m_\sigma \to \infty$ requires the constraint

$$E_{\rm CON}(M;\chi,b_1)\equiv 0 \tag{19}$$

as a necessary condition for the existence of physical solutions. In our actual calculations we were able to satisfy (19) numerically thanks to the fact that $E_{\rm CPL}$ and $E_{\rm INF}$ have opposite phases. Figure 2 shows two examples of the $E_{\rm CON}\equiv 0$ line in the (χ,b_1) plane for fixed values of the parameter M.

Technically, Eq. (19) may be regarded as an implicit definition of χ as a function of M and b_1. We can insert $\chi=\chi(M;b_1)$ into $E(M,\chi,b_1)$, i.e., the right-hand side of (7) with the entire Hamiltonian (8a), and obtain this energy as a function of M and b_1 only. Let us employ

$$E(M;b_1)=E(M;\chi(M,b_1),b_1) \tag{20}$$

as a compact notation. On this quantity hinges the variational procedure: In terms of $E(M;b_1)$ the equation for the soliton rest mass, (7) and (17), reads

$$M=E(M;b_1)\,. \tag{21}$$

This equation may be viewed in turn as an implicit definition of the function $M=M(b_1)$ and now requires that M be a minimum with respect to the trial parameter b_1, in particular,

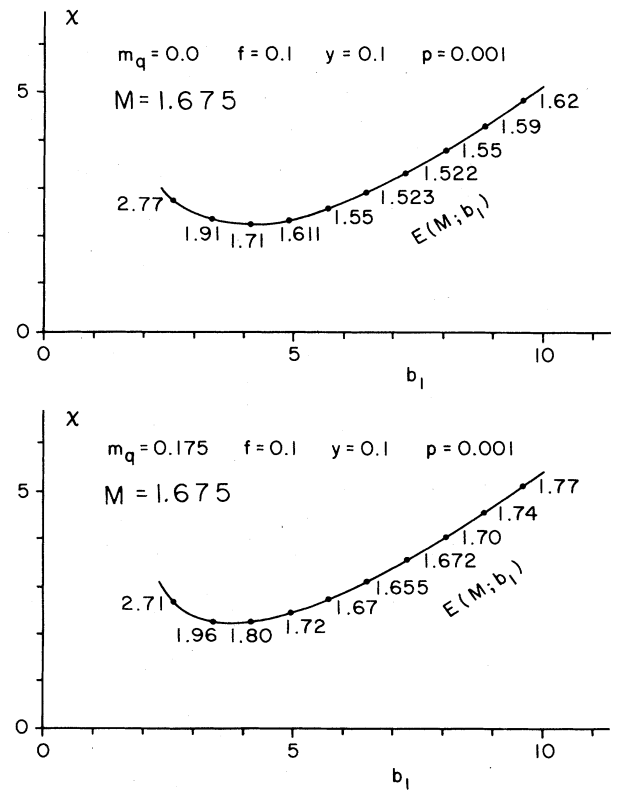

FIG. 2. The curves satisfy the equation $E_{\rm con}(M;\chi,b_1)=0$. We show two examples for $m_q=0$ and $m_q=0.175$ GeV. In both cases we fix $M=1.675$ GeV. The values identifying the various points on the curve are those of the corresponding energy $E(M;b_1)$.

$$\frac{dM}{db_1}=0 . \tag{22}$$

If we apply this condition to (21), i.e.,

$$\frac{dM}{db_1}=\frac{\partial E}{\partial M}\frac{dM}{db_1}+\frac{\partial E}{\partial b_1} \tag{23}$$

it follows that

$$\frac{\partial E(M;b_1)}{\partial b_1}=0 . \tag{24}$$

Equations (21) and (24) show how to calculate b_1 and M. Obviously, similar equations hold in case we are dealing with more than one variational parameter.

In practice, we have chosen a fixed starting value for M and, according to (24), determined numerically the minimum of $E(M;b_1)$ with respect to b_1 on the $E_{\rm CON}=0$ line. This is illustrated, again, in Fig. 2 by the actual energies $E(M,b_1)$ which satisfy the $E_{\rm CON}=0$ condition. The minimum $E(M;b_1)$, in these examples, is different from the starting value for M. In order to simultaneously satisfy (24) and (21), the minimum $E(M;b_1)$ with respect to b_1 is found on the $E_{\rm CON}=0$ line and this is followed by a search for M such that the self-consistency condition $M-E(M)=0$ is satisfied as well as Eqs. (19) and (24).

All of our results presented in the subsequent section have been calculated at the self-consistency point, i.e., satisfying Eqs. (19), (21), and (24). In the figures this is indicated by $M=E(M)$.

In the Appendix we present the explicit form of the results for the normalization (overlap) Eq. (6) and the Hamiltonian matrix elements Eq. (8) that enter in Eq. (17), using the ansatz Eqs. (3), (9), (10), (11), (14), and (16).

IV. RESULTS AND DISCUSSION

According to the scaling property of the model, all dimensional quantities are given in units of an appropriate power of ϵ_1. We have fixed $\epsilon_1=1$ GeV.

A convenient measure for the characteristic size of the vacuum bubble is the distance R_b from its center to where the vacuum expectation value of the σ field is one half of its value in the normal vacuum. Using the ansatz (16) in formula (24b) of I, we find

$$\langle v\,|\,\sigma(x)\,|\,v\rangle=f-\sqrt{2}\chi\epsilon_1(\pi\epsilon_1 b_1^{\,2})^{-3/2}e^{-x^2/2b_1^{\,2}} . \tag{25}$$

The condition $\langle v\,|\,\sigma(\chi)\,|\,v\rangle=f/2$ at $|\vec{x}|=R_b$ then leads to the definition

$$R_b=\left[2b_1^{\,2}\ln\frac{2\sqrt{2}\chi}{(f/\epsilon_1)(\pi\epsilon_1^{\,2}b_1^{\,2})^{3/4}}\right]^{1/2} . \tag{26}$$

We will refer to R_b as the bubble radius.

A conventional measure for the size of the quark distribution is the root-mean-square radius R_q. Using our ansatz (14) together with the condition $\omega_0=M/3$ yields

$$R_q=\sqrt{3/2}\,b_0\left[\frac{(M/3+m_q)^2b_0^{\,2}+5/2}{(M/3+m_q)^2b_0^{\,2}+3/2}\right]^{1/2}$$
$$=\left[\frac{9M/3-m_q}{7M/3+m_q}\frac{3}{(M/3)^2-m_q^{\,2}}\right]^{1/2} . \tag{27}$$

Thus the dynamical features enter into R_q via the self-consistent soliton mass $M=E(M)$.

As a final preliminary remark, we remind the reader that all our results for dynamically calculated quantities, namely, M,χ,b_1 and thus also b_0,R_b,R_q, correspond to the limit of infinite m_σ and g, see Sec. III. Therefore we are left with only four model parameters y, f, m_q, and p, and we display results in terms of these parameters in Figs. 3–6.

We begin by showing in Fig. 3(a) the dependence of $M=E(M)$, χ, b_0, b_1, R_b, and R_q on the parameter y for the fixed values $f=0.100$ GeV, $m_q=0.0$, and $p=0.001$ GeV^4 ($p^{1/4}=0.178$ GeV). Note that each curve is assigned an individual scale. The size of the quark distribution and the size of the vacuum bubble differ by a remarkably large amount. The ratio of b_0 and b_1, and also R_q and R_b, is of the order $\frac{2}{3}$ to $\frac{1}{2}$. The quarks occupy only a relatively small portion in the vacuum bubble. This feature is apparent in all our results. It is expected however that in the chiral version of our model, the pion field will shrink R_b to smaller values.

According to the definition (13), a larger value of y essentially means that (with other parameters kept fixed) the coupling between the quarks and the σ field becomes more attractive and, as Fig. 3 shows, the radii R_q and R_b tend to come closer together as y increases. The bubble narrows and the quark distribution expands somewhat within the bubble. As a consequence of the increasing quark radius R_q, the quark kinetic energy $E_{\rm DIR}$ decreases. This is the reason behind the slight reduction in the rest mass $M=E(M)$. The absolute values of $E_{\rm CPL}$ and $E_{\rm POT}$ increase, but being of opposite sign and nearly equal in magnitude, their sum is of little consequence for the value of $E(M)$. In quantitative terms, however, our variational solution behaves rather insensitively to y. The rest mass, for instance, remains almost stable around 1.250 GeV for the displayed range of y.

We observe very similar trends in Fig. 3(b) for a quark mass $m_q=0.175$ GeV. This value m_q is the strange-quark mass resulting from the experimental nucleon-Λ mass difference in the naive constituent quark model. The radius R_q of the quark distribution has now decreased to about 0.75 fm while the soliton mass M has increased to approximately 1.6 GeV. Thus M has gained only about 0.350 GeV whereas a mass of $3\times m_q=0.525$ GeV was originally added to the system. Clearly this effect is due to the nontrivial dynamics in our quark-σ field and, in particular, reflects the competition between the different contributions to the total energy $E(M)$.

In all subsequent calculations we have fixed $y=0.1$. In order to get a feeling for this value, we note that, according to (13), it is reproduced, e.g., by $m_\sigma=10$ GeV and $gf=10$ GeV for the σ-mass and the outside quark mass, respectively; the coupling constant then is $g=100$.

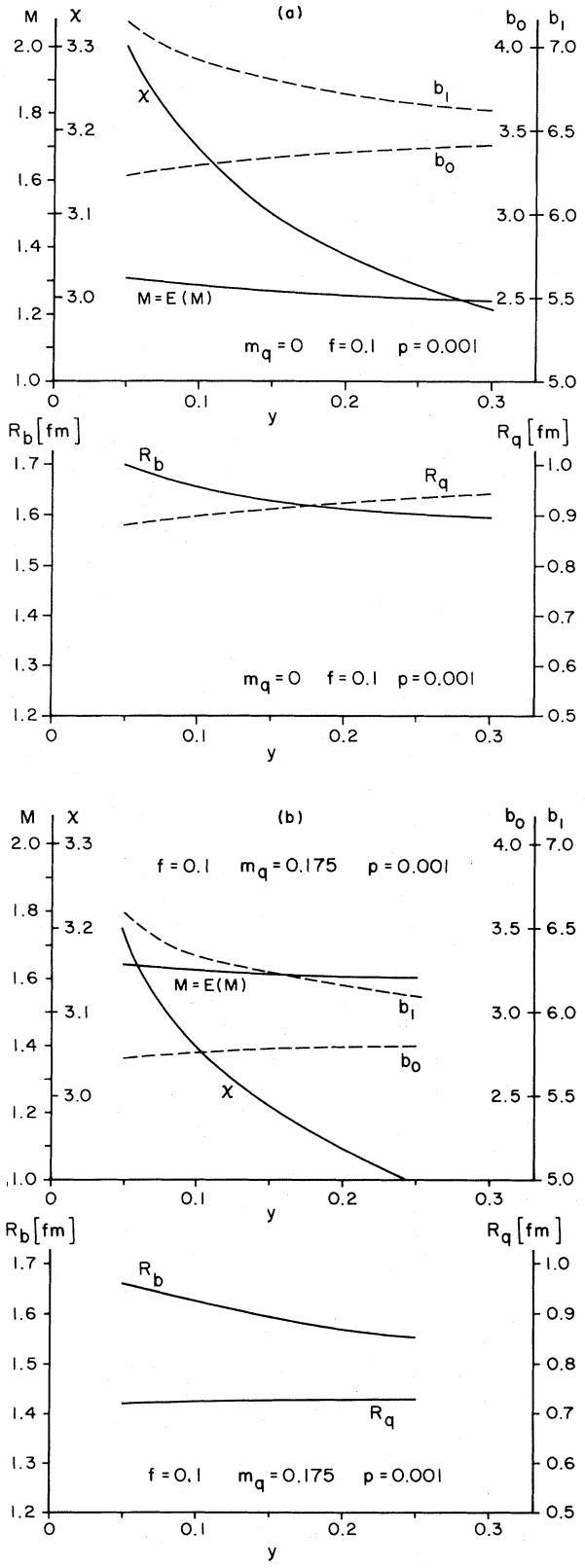

FIG. 3. (a) The self-consistent mass $M=E(M)$ and dynamical variables χ, b_0, b_1 and the radii R_b and R_q as a function of y. b_0 is found from Eq. (14c). Note that each quantity is assigned a different scale and that $m_q=0.0$. (b) The same quantities as in (a) but for $m_q=0.175$ GeV.

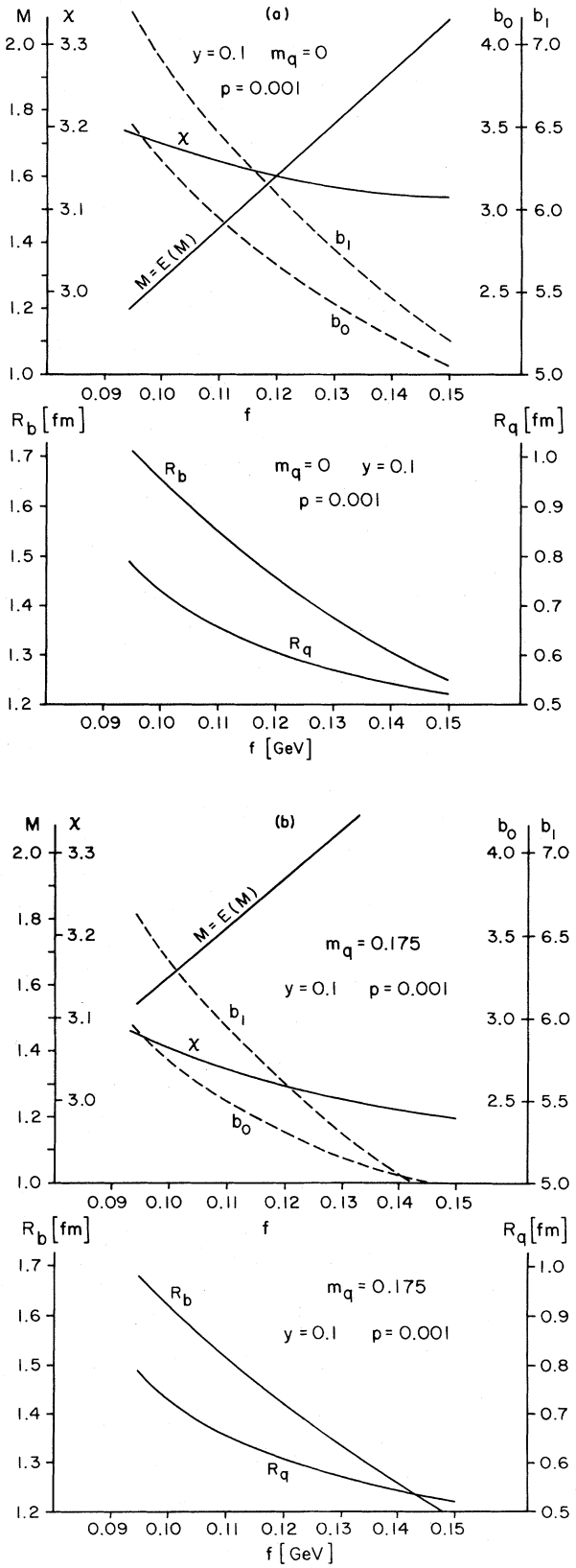

FIG. 4. (a) The self-consistent mass $M=E(M)$ and dynamical variables and radii as a function of the asymptotic value f of the σ field. Note that $m_q=0.0$. (b) The same quantities as in (a) but for $m_q=0.175$ GeV.

In Figs. 4(a) and 4(b) we show the dependence of M, χ, b_0, b_1, R_b, and R_q on the expectation value f of the σ field in the normal vacuum, again, for two different quark masses m_q. We observe a much stronger dependence of these variables on f except for the bubble depth parameter χ which remains substantially constant. In particular the sensitivity of $M=E(M)$ with regard to f is rather dramatic. If we also allow m_q to vary, we can cover the entire mass range of physically important baryon resonances, say 1.1—1.8 GeV, with a change in f by only about 25%. This effect provides us with the means for determining the physical value at f with relatively high precision from baryon mass fits provided m_q is known. Note that f is not very accurately known in the strange sector; we may expect it to be somewhere in the range 0.09—0.15 GeV. As to the radii, we see in Figs. 4(a) and 4(b) that larger values of f cause a sizable decrease of b_0, b_1 and R_b, R_q. As the bubble becomes narrower, the Dirac kinetic energy increases and thus contributes to the rapid increase of M. As usual R_q remains substantially smaller than R_b (note the different scales in Fig. 4).

We now come to a more detailed examination of the role of the quark mass m_q in the soliton system. As anticipated $M=E(M)$ increases with m_q, not only because the quarks become more massive but also because their kinetic energy increases at the same time. In fact the net change in $E(M)$ is due almost entirely to that of $E_{\rm DIR}$ while $E_{\rm SIG}$ and $E_{\rm CPL}+E_{\rm POT}$ remain almost unchanged in the range of m_q shown in Fig. 5. The radii R_b and R_q remain also fairly constant, R_b more so than R_q. The general trend revealed by Fig. 5 is that the soliton system reacts to an increase of the quark mass by narrowing the quark distribution in a bubble of fairly constant width.

The last of our model parameters is the strength p of the potential $V(\sigma)$ at $p=0$. The quantity p has a somewhat similar interpretation as the volume energy density parameter in the MIT model. The value $p=0.001$ GeV^4 (adopted for all the rest of our calculations) corresponds to $p^{1/4}=0.178$ GeV and $p=0.13$ GeV fm^{-3}, in customary units. It was difficult to find solutions to Eq. (25) beyond the range of p shown in Fig. 6. Within this interval, however, we again see that the mass of the soliton and the sizes of the bubble and quark distribution remain remarkably constant. This qualitative behavior is not affected by changing the value of m_q.

From the examination of Figs. 3—6 we conclude that among all the model parameters only f and m_q can effectively influence the soliton characteristics. For all practical purposes we may choose $y=0.1$ and $p=0.001$ GeV^4 and proceed to make contact with the phenomenology of hadrons. It is appropriate now to estimate the errors introduced into the calculation of baryon masses due to violation of translational invariance. Figure 7 shows that the Dirac energy $E_{\rm DIR}$ contributing to the self-consistent mass, Eq. (7), is the dominant term; therefore, it suffices as a check on the effects of our projection formalism. In the absence of boosts and momentum projections, i.e., $\Pi_k U(\Lambda_k)$ in Eq. (3), $E_{\rm DIR}$ reduces to

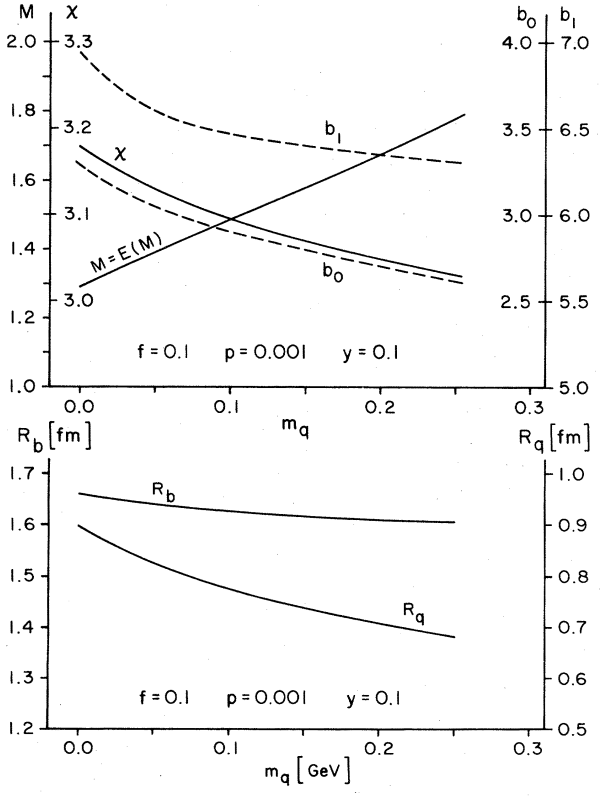

FIG. 5. The self-consistent mass $M=E(M)$ and dynamical variables and radii as a function of the quark mass m_q for $f=0.1$.

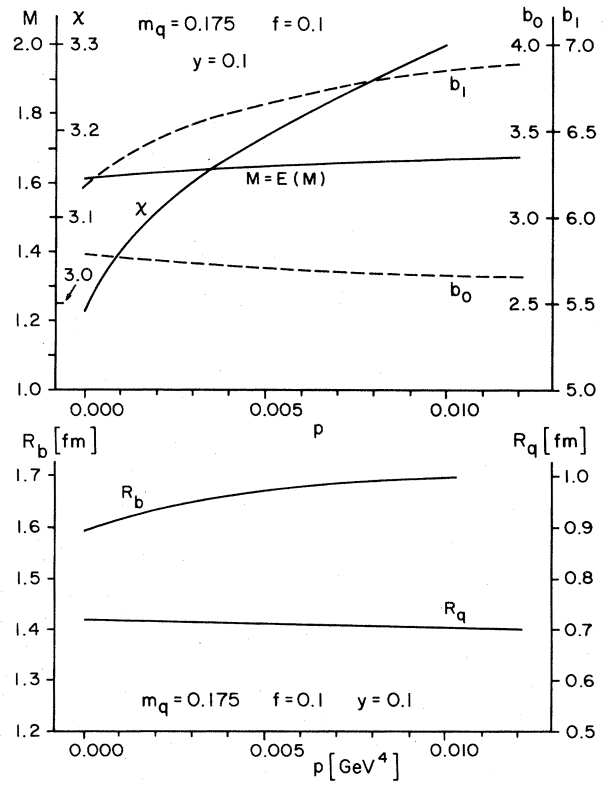

FIG. 6. The self-consistent mass $M=E(M)$ and dynamical variables and radii as a function of the potential parameter p.

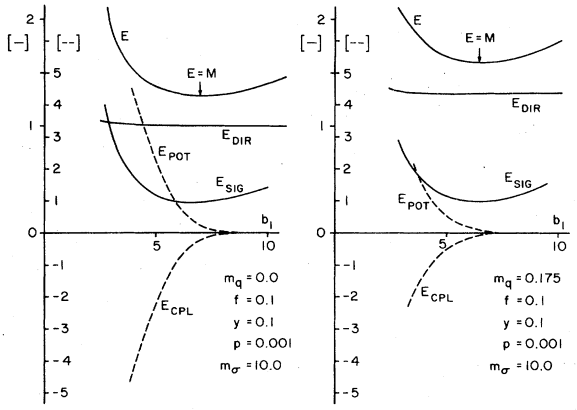

FIG. 7. The four contributions $E_{\rm DIR}$, $E_{\rm POT}$, $E_{\rm SIG}$, and $E_{\rm CPL}$ to the energy $E(M)$ shown as a function of b_1. The self-consistent mass $M=E(M)$ is indicated by an arrow in the $E(M)$ curve. We note that $E(M)$ is quite stable about the minimization value of b_1 where $M=E(M)$. These results do not change for $m_\sigma \gg 10$ GeV.

$$E_{\rm DIR}^{\rm static}=3\int d^3x\,\bar{u}_0(x)\left[-\frac{i}{2}\gamma\cdot\overleftrightarrow{\nabla}+m_q\right]u_0(x)$$

$$=3n_0{}^2\left[\frac{3}{2}\frac{2-m_q/(\omega_0+m_q)}{(\omega_0+m_q)b_0{}^2}+m_q\right]. \qquad (28)$$

In Table II we show the percent deviation of $E_{\rm DIR}$ from $E_{\rm DIR}^{\rm static}$ for four different values of the quark mass m_q. We note substantial discrepancies ranging from 11 to 14%.

Once the self-consistent mass $M=E(M)$ has been found, we can check the stability of the system with respect to changes in the variational parameters. In Fig. 7, we show the total energy $E=E(M,b_1)$, with M being fixed at the self-consistency point, as a function of b_1. Again we consider two different quark masses $m_q=0.0$ and $m_q=0.175$ GeV. We note that in both cases the minima are rather shallow, a feature which is similar in the MIT model. In Fig. 7 we have also displayed the individual contributions to the total energy E, according to the decomposition (8). We see that $E_{\rm DIR}$ remains rather flat whereas $E_{\rm SIG}$ behaves like E itself although $E_{\rm SIG}$ contributes only about 25%, or less, to the total energy. The condition imposed by Eq. (19) results in an almost complete cancellation of $E_{\rm CPL}+E_{\rm POT}$, so that the rapid change in these latter quantities does not affect the stability of E at the minimum. Unlike our other results, the display of $E_{\rm CPL}$ and $E_{\rm POT}$ requires a finite choice for the σ mass. We have taken $m_\sigma=10$ GeV which should be large enough to encompass the correct physics of the system. Consequently $E_{\rm CPL}$ and $E_{\rm POT}$ are both very large in magnitude (note the different scales in Fig. 7) and the finite part of the latter, see Eqs. (12), is dominated by the piece proportional to $m_\sigma{}^2$. These results do not change if we let $m_\sigma \gg 10$ GeV.

TABLE II. The Dirac energy of the quarks in the projection formalism ($E_{\rm DIR}$) and in the absence of boosts and momentum projections ($E_{\rm DIR}^{\rm static}$) and the % deviation between the two. Masses and energies in GeV. ($Y=0.1$, $p=0.001$, $m_\sigma=10$ GeV.)

m_q	f	$M=E(M)$	$E_{\rm DIR}$	$E_{\rm DIR}^{\rm static}$	% deviation
0	0.11	1.681	1.263	1.441	14.0
	0.095	1.417	1.072	1.215	13.4
0.175	0.11	1.957	1.516	1.767	12.6
	0.095	1.715	1.345	1.502	11.7
0.225	0.11	2.048	1.607	1.798	11.9
	0.095	1.812	1.442	1.600	11.0

It should be pointed out that the physical energies are in fact energy differences between the quark-bag state and the normal vacuum. At the present level of approximation, disregarding time-dependent quantum fluctuations, the vacuum energy can be obtained by calculating the energy matrix element between the states $|v\rangle$, Eqs. (11) and (16), in the absence of quarks. It turns out that the total energy functional calculated from (17) has an absolute minimum at $M=0$. This occurs at the value $\chi=0$ for the bubble depth parameter. Hence the empty bag collapses to the normal vacuum $\langle\sigma\rangle=f$ with zero energy. For example, the contribution from the σ field is

$$E_{\rm SIG}=\chi^2[\tfrac{3}{2}(b_1\epsilon_1)^{-2}\epsilon_1]\underset{\chi\to 0}{\to}0\,.$$

V. CONCLUSIONS

We have found (approximate) solutions for the rest mass and the radius of the soliton in our model within a range that is eminently satisfactory vis-a-vis the experimental results for the ground-state baryons. The freedom furnished by the parameters f and m_q can be utilized to achieve agreement with the data. To proceed further we need to implement chiral symmetry and gluon radiation. Chiral symmetry may be realized by including pion fields $\pi^0,\pi^\pm$ along with the chiral partner, the σ field, in the description of the bubble. The present framework has still to be extended in this sense. However, we can apply our model to the simplest of all baryons, namely, the Ω^- which being composed of three strange quarks would have no interaction with the pion field, provided we incorporate the gluon-exchange energy in the calculation of $E(M;b_1)$.

For the present purpose it is sufficient to use the expression for the color-magnetic energy evaluated in the MIT bag model because we are dealing with a very similar physical situation when $g,m_\sigma{}^2\to\infty$. Thus, let us add to $E(M;b_1)$ the energy

$$E_c=3(0.1769-0.0474\zeta+0.0038\zeta^2)\left[\frac{8\alpha_c}{3R}\right], \qquad (29)$$

which is a parametric form of the MIT result for the magnetic energy;[1] $\zeta=m_qR$ and the coupling parameter is $\alpha_c=0.55$. For R we take the rms radius R_q as given by Eq. (27) in terms of M and m_q. We have now repeated the variational calculation precisely as explained above but including E_c, again with $y=0.1$ and $p=0.001$ GeV^4. The results are shown in Fig. 8. The figure displays families of curves corresponding to different values of m_q.

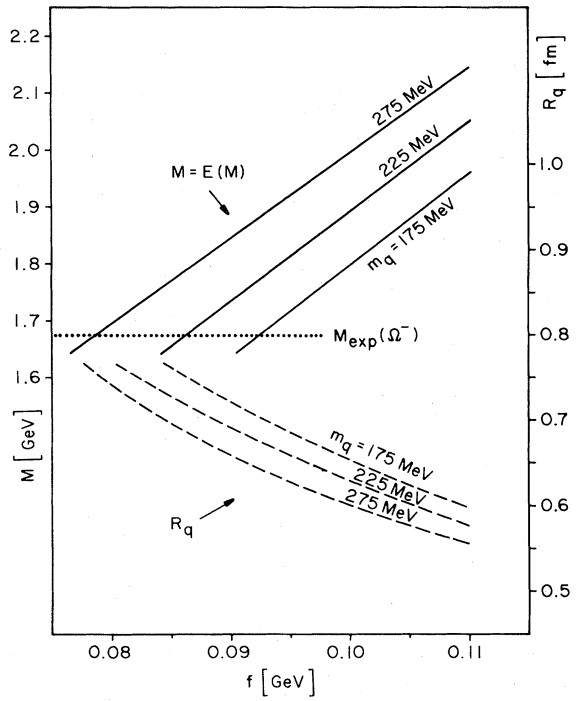

FIG. 8. The results of the variational calculation for $M=E(M)$ and R_q, including the color-magnetic energy, Eq. (29), as a function of f and for various quark masses m_q. Recall that f and m_q are the two parameters on which $M=E(M)$ depends sensitively.

For each one, the self-consistent rest mass M and the quark rms radius R_q are plotted as a function of f. For a given value of f, the bubble width R_b is essentially the same for all m_q. The color-magnetic energy is of the order of 60—70 MeV. At the experimental Ω^- mass, i.e., 1.675 GeV, we find the radius of the quark distribution as shown in Table III. It is encouraging to see the results come out in so close agreement with other analyses.[9] Of course, we have the advantage that our results are free from spurious center-of-mass excitations (except for c.m. corrections to E_c which should be negligible).

By using one more experimental result in addition to the rest mass M, such as the magnetic moment of the Ω^-, we could determine the values of f, m_q, and also the radii of the quark distribution and the vacuum bubble.

A final remark is in order regarding our variational space. We have attempted to use trial functions for the quark spinor and the bubble function which are as good a guess as possible. In principle, of course, each extension of the variational space of trial functions will result in a somewhat smaller value for the rest mass M. One might suspect that the Gaussian ansatz (16) should be the first candidate for an improvement (by polynomials, say). These questions cannot be answered without further calculations. However, we have been able to perform some numerical tests where both b_0 and b_1 were independent variational parameters. The results seem to indicate that we might have to expect a decrease in M about the order of magnitude of the color-magnetic energy. Such a smaller value would be very easy to compensate for because of

TABLE III. Soliton parameters at the experimental mass of the Ω^-, $M=1.675$ GeV, for the three values of m_q.

f (MeV)	m_q (MeV)	R_q (fm)	R_b (fm)
95	175	0.70	1.69
87	225	0.72	1.79
78	275	0.75	1.92

the relatively high sensitivity of M to the parameters m_q and especially f.

In conclusion, the translationally invariant soliton bag model that we developed in I manifests a great deal of versatility in the present calculation of the soliton rest mass. We have demonstrated that our solutions are stable over a reasonably wide range of the dynamical parameters of the model. Our results for the rest mass span the range of ground-state hadronic masses and those for the radius of the quark distribution agree with results of other authors employing different methodologies [(9) and (10)]. The advantage of our formalism is that it has no ambiguities arising from violation of translational invariance. This feature is a necessity in calculations of hadronic form factors, but it is also important in calculations of static properties as in the present case, as was demonstrated in Sec. III. The present model can be generalized to include baryons with a pion cloud when chiral properties are incorporated; also when the gluon-exchange processes are taken into account more rigorously than it was done in the present exploratory calculation.

ACKNOWLEDGMENTS

This work was supported by the National Science Foundation under Contract No. PHY-82-07-046, the United States Department of Energy under Contract No. DEAC02-76ER13001, and the Research Foundation of the State of New York and in part by the Heinrich-Hertz-Stiftung des Landes NRW. One of the authors (E.H.) wishes to thank the Physics Department of Yale University for their hospitality during a vist, on which this work was done.

APPENDIX

We list here the overlap and Hamiltonian matrix elements as they occur in formula (17) with the particular choices (14) and (16) for the trial functions.

As common abbreviations we use

$$\Lambda^3=(2\pi)^{-3}(h\mid\mathscr{A}\mid h)\left[1+\frac{3}{2\nu_0^2}\right]^{-3}(\pi\beta_1^2)^{3/2},$$

$$\nu_0=(\omega_0+m_q)b_0,$$

$$\frac{1}{\beta_l^2}=\frac{3}{4b_0^2}+\frac{l}{4b_1^2},\quad l=0,1,\ldots,\infty$$

where $(h\mid\mid h)$ is defined in Eq. (49b) of I. Note that the factor $\delta(M-3\omega_0)$ drops out from the quotient of formula

(17). In all our calculations we have used

$$\chi_l = e^{-\chi^2/2}(-\chi)^l, \quad l=0,1,\ldots,\infty$$

although in the formulas given below no advantage has been taken of this particular form.

(a) Normalization:

$$\langle v \mid B_0 \Pi_{(M,\vec{0})} B_0^\dagger \mid v \rangle = \delta(M-3\omega_0)\Lambda^3 \sum_{l=0}^{\infty} \frac{1}{l!}\chi_l{}^2 \sum_{k=0}^{3} \begin{bmatrix} 3 \\ k \end{bmatrix} (2k+1)!!2^{-k} \left[\frac{\beta_l}{2b_0}\right]^{2k} \left[\frac{\beta_l}{\beta_1}\right]^3 (-)^k \left[1+\frac{3}{2\nu_0{}^2}\right]^{3-k} \nu_0{}^{-2k} . \tag{A1}$$

(b) Dirac energy:

$$\langle v \mid B_0 \Pi_{(M,\vec{0})} H_{\mathrm{DIR}} B_0^\dagger \mid v \rangle = \delta(M-3\omega_0)\Lambda^3 \frac{3}{b_0} \sum_{l=0}^{\infty} \frac{1}{l!}\chi_l{}^2 \sum_{k=0}^{3} \begin{bmatrix} 3 \\ k \end{bmatrix} (2k+1)!!2^{-k} \left[\frac{\beta_l}{2b_0}\right]^{2k} \left[\frac{\beta_l}{\beta_1}\right]^3 (-)^k T_k , \tag{A2}$$

with

$$T_0 = t s_+{}^2, \quad T_1 = \frac{1}{3\nu_0} s_+ \left[\frac{2t}{\nu_0} + r s_+\right], \quad T_2 = \frac{1}{3\nu_0{}^3}\left[\frac{t}{\nu_0} + 2r s_+\right], \quad T_3 = \nu_0{}^{-5} r ,$$

and

$$r = 2 - \frac{m_q b_0}{\nu_0}, \quad s_+ = 1 + \frac{3}{2\nu_0{}^2}, \quad t = \frac{3}{2\nu_0{}^2}\left[2 - \frac{m_q b_0}{\nu_0}\right] + m_q b_0 .$$

(c) σ field energy:

$$\begin{aligned} \langle v \mid B_0 \Pi_{(M,\vec{0})} H_{\mathrm{SIG}} B_0^\dagger \mid v \rangle &= \delta(M-3\omega_0)\Lambda^3 (2\epsilon_1)^{-1} \frac{3}{2b_1{}^2} \sum_{l=0}^{\infty} \frac{1}{l!} \sum_{k=0}^{3} \begin{bmatrix} 3 \\ k \end{bmatrix} (2k+1)!!2^{-k} \left[\frac{\beta_l}{2b_0}\right]^{2k} \left[\frac{\beta_l}{\beta_1}\right]^3 (-)^k \left[1+\frac{3}{2\nu_0{}^2}\right]^{3-k} \nu_0{}^{-2k} \\ &\quad \times \left\{ \chi_l \chi_{l+2} + \left[\frac{\beta_{l+1}}{\beta_l}\right]^{2k+3} \left[1 - \frac{2k+3}{12}\left[\frac{\beta_{l+1}}{b_1}\right]^2\right] \chi_{l+1}{}^2 \right\} . \end{aligned} \tag{A3}$$

(d) Coupling energy:

$$\begin{aligned} \langle v \mid B_0 \Pi_{(M,\vec{0})} H_{\mathrm{CPL}} B_0^\dagger \mid v \rangle &= \delta(M-3\omega_0)\Lambda^3 3g \sum_{l=0}^{\infty} \frac{1}{l!} \sum_{k=0}^{3} \begin{bmatrix} 3 \\ k \end{bmatrix} (2k+1)!!2^{-k} \left[f \chi_l{}^2 C_k \left[\frac{\beta_l}{2b_0}\right]^{2k} \left[\frac{\beta_l}{\beta_1}\right]^3 \right. \\ &\quad \left. + (2\epsilon_1)^{-1/2} (\pi b_1{}^2)^{-3/4} \chi_l \chi_{l+1} D_k \left[\frac{\gamma_l}{2b_0}\right]^{2k} \left[\frac{\gamma_l}{\beta_1}\right]^3 \right] , \end{aligned} \tag{A4}$$

with

$$\frac{1}{\gamma_l{}^2} = \frac{1}{\beta_l{}^2} + \frac{1}{4(b_0{}^2+2b_1{}^2)} ,$$

further

$$C_0 = s_+{}^2 s_-, \quad C_1 = \tfrac{1}{3} s_+ \nu_0{}^{-2}(s_+ - 2s_-), \quad C_2 = \tfrac{1}{3}\nu_0{}^{-4}(s_- - 2s_+), \quad C_3 = \nu_0{}^{-6} ,$$

$$D_0 = w s_+{}^2 p, \quad D_1 = \tfrac{1}{3} w (s_+ q - 2\nu_0{}^{-2} p) s_+, \quad D_2 = \tfrac{1}{3} w (\nu_0{}^{-4} p - 2 s_+ \nu_0{}^{-2} q), \quad D_3 = w \nu_0{}^{-4} q ,$$

and

$$s_\pm = 1 \pm \frac{3}{2\nu_0{}^2}, \quad w = 2\left[1 + \frac{b_0{}^2}{2b_1{}^2}\right]^{-3/2} ,$$

$$p = 1 - \nu_0{}^{-2} 3 b_1{}^2 (b_0{}^2 + 2b_1{}^2)^{-1}, \quad q = \nu_0{}^{-2} 4 b_1{}^2 (b_0{}^2 + b_1{}^2)(b_0{}^2 + 2b_1{}^2)^{-2} .$$

(e) Potential energy: For an arbitrary potential with Taylor expansion

$$V(\sigma) = \sum_{K=1}^{\infty} \frac{1}{K!} V^{(K)}(f)(\sigma - f)^K ,$$

the matrix element is

$$\langle v \mid B_0 \Pi_{(M,\vec{0})} H_{\rm POT} B_0^\dagger \mid v \rangle = \delta(M-3\omega_0)\Lambda^3 \sum_{K=1}^{\infty} \frac{1}{K!} V^{(K)}(f)(2\epsilon_1)^K (4\pi\epsilon_1{}^2 b_1{}^2)^{-3K/4} \left[\frac{2\pi b_1{}^2}{K}\right]^{3/2} \times \sum_{l=0}^{\infty} \frac{1}{l!} \sum_{i=0}^{K} \begin{bmatrix} K \\ i \end{bmatrix} \chi_{l+i}\chi_{l+(K-i)} \left[\frac{\alpha_{l,Ki}}{\beta_1}\right]^3 \times \sum_{k=0}^{3} \begin{bmatrix} 3 \\ k \end{bmatrix} (2k+1)!!2^{-k}(-)^k \left[1+\frac{3}{2\nu_0{}^2}\right]^{3-k} \nu_0{}^{-2k} \left[\frac{\alpha_{l,Ki}}{2b_0}\right]^{2k}, \tag{A5}$$

with

$$\frac{1}{\alpha_{l,Ki}{}^2} = \frac{1}{\beta_l{}^2} + \frac{i(K-i)}{2Kb_1{}^2} .$$

The K sum is usually small, $K=1,\ldots,4$.

The only infinite sum which occurs in the previous formulas is the l sum. For, typically, $\chi \gtrsim 3$ only few terms are needed.

*Permanent address: Dept. of Physics, Florida International University, Miami, Florida 33199.

†Permanent address.

[1]A. Chodos, R. L. Jaffe, K. Johnson, C. B. Thorn, and V. F. Weisskopf, Phys. Rev. D **9**, 3471 (1974); T. DeGrand, R. L. Jaffe, K. Johnson, and J. Kiskis, *ibid.* **12**, 2060 (1975).

[2]G. E. Brown, M. Rho, and V. Vento, Phys. Lett. **97B**, 423 (1980); V. Vento *et al.*, Nucl. Phys. **A345**, 413 (1980); S. Theberge, A. W. Thomas and G. A. Miller, Phys. Rev. D **22**, 2838 (1980).

[3]I. Picek and D. Tadić, Phys. Rev. D **20**, 723 (1979); W-Y.P. Huang, Z. Phys. C **16**, 327 (1983).

[4]J. L. Dethier, R. Goldflam, E. M. Henley, and L. Wilets, Phys. Rev. D **27**, 2191 (1983).

[5]H. R. Fiebig and E. Hadjimichael, preceding paper, Phys. Rev. D **30**, 181 (1984).

[6]T. D. Lee, *Particle Physics and Introduction to Field Theory* (Academic, New York, 1981); R. Friedberg and T. D. Lee, Phys. Rev. D **15**, 1694 (1977); **18**, 2623 (1978).

[7]R. E. Peirls and J. Yoccoz, Proc. Phys. Soc. London **A70**, 381 (1957).

[8]M. Bolsterli, Phys. Rev. D **13**, 1727 (1976).

[9]F. Myhrer, Phys. Lett. **110B**, 353 (1982).

[10]M. Betz and R. Goldflam, Phys. Rev. D **28**, 2848 (1983).